Stem Cell Reviews and Reports (2023) 19:430–442
https://doi.org/10.1007/s12015-022-10431-y

Derivation of Human Salivary Epithelial Progenitors from Pluripotent Stem Cells via Activation of RA and Wnt Signaling

Siqi Zhang[1,2] · Yi Sui[1] · Yifei Zhang[1] · Shuang Yan[1] · Chong Ding[1] · Yanrui Feng[1] · Jingwei Xiong[2] · Shicheng Wei[2,3]

Accepted: 17 July 2022 / Published online: 10 August 2022
© The Author(s), under exclusive licence to Springer Science+Business Media, LLC, part of Springer Nature 2022

Abstract

Derivation of salivary gland epithelial progenitors (SGEPs) from human pluripotent stem cells (hPSCs) has great potential in developmental biology and regenerative medicine. At present, no efficient method is available to generate salivary gland cells from hPSCs. Here, we described for the first time a robust protocol for direct differentiation of hPSCs into SGEPs by mimicking retinoic acid and Wnt signaling. These hPSC-derived SGEPs expressed SOX9, KRT5, and KRT19, important progenitor markers of developing salivary glands. CD24 and α-SMA positive cells, capable of restoring the functions of injured salivary glands, were also present in SGEP cultures. Importantly, RNA-sequencing revealed that the SGEPs resembled the transcript profiles of human fetal submandibular glands. Therefore, we provided an efficient protocol to induce hPSCs differentiation into SGEPs. Our study provides a foundation for generating functional hPSCs derived salivary gland acinar cells and three-dimensional organoids, potentially serving as new models for basic study and future translational research.

Keywords Human pluripotent stem cells · Differentiation · Salivary glands · Progenitors · Protocol

Introduction

Generation of tissue-specific cells from human pluripotent stem cells (hPSCs), including human embryonic stem cells (hESCs) and human induced pluripotent stem cells (hiPSCs), overcomes the ethical limitations in the study of human organ development and are considered valuable resources for regenerative medicine [1–6]. Three major salivary glands (SGs), such as submandibular glands (SMGs), and several minor SGs, produce and secrete saliva into the mouth [7]. Saliva is essential for digestion and maintenance of oral health. Most known signaling pathways involving SG organogenesis are obtained from mouse models [8], and limited knowledge is available about the regulatory mechanism underlying human SG development. Additionally, SG hypofunction caused by therapeutic radiation for head and neck cancer is extremely common and significantly impairs patients' quality of life and general health status [7, 9]. Large-scale production of human SG cells with regenerative potential may allow restoration of the injured SG structure and function. However, to our knowledge, no efficient protocol has been developed for direct differentiation of hPSCs into SG cells.

SGs are derived from oral ectoderm (OE), and their development begins at embryonic day 11 (E11) in mice and 6-8 weeks in humans [10]. Studies of mouse models have revealed that SG development requires interaction between epithelium and underlying mesenchyme, which involves multiple signaling pathways and transcription factors [11, 12]. SOX9 is the earliest known transcription factor of the SG epithelium. SOX9 positive cells are located in the distal initial-buds in the early stages, and remain throughout SG development. Disruption of the SOX9 gene results in the loss of the distal epithelial progenitors and a failure in forming normal SMGs [13]. A previous study revealed that overexpression of SOX9 promotes the differentiation of salivary rudiments from mouse embryonic stem cells [14]. Furthermore, retinoic acid (RA) signaling plays an important role in regulating initial mouse SMG development [15].

✉ Shicheng Wei
sc-wei@pku.edu.cn

1 Central Laboratory, and Department of Oral and Maxillofacial Surgery School and Hospital of Stomatology, Peking University, Beijing 100081, China

2 Institute of Molecular Medicine, Peking University, Beijing 100871, China

3 Laboratory of Biomaterials and Regenerative Medicine, Academy for Advanced Interdisciplinary Studies, Peking University, Beijing 100871, China

Conditional mutation of RA signaling in OE failed to initiate SMG organogenesis, including thickening and invagination to form the initial-buds. Of note is that the expression of SOX9 is dependent on RA signaling during SMG organogenesis [16]. Additionally, Wnt/β-catenin-dependent signaling is active in the mouse SMG mesenchyme around the initial-buds (E12-15) and decreases during development. Wnt signaling controls the timing of SMG development by maintaining the initial-bud progenitors in an undifferentiated bipotent state [17]. Therefore, we assume that Wnt signaling is essential after SG initiation. However, it is not clear whether these signaling pathways participate in the differentiation of human SG epithelial progenitors.

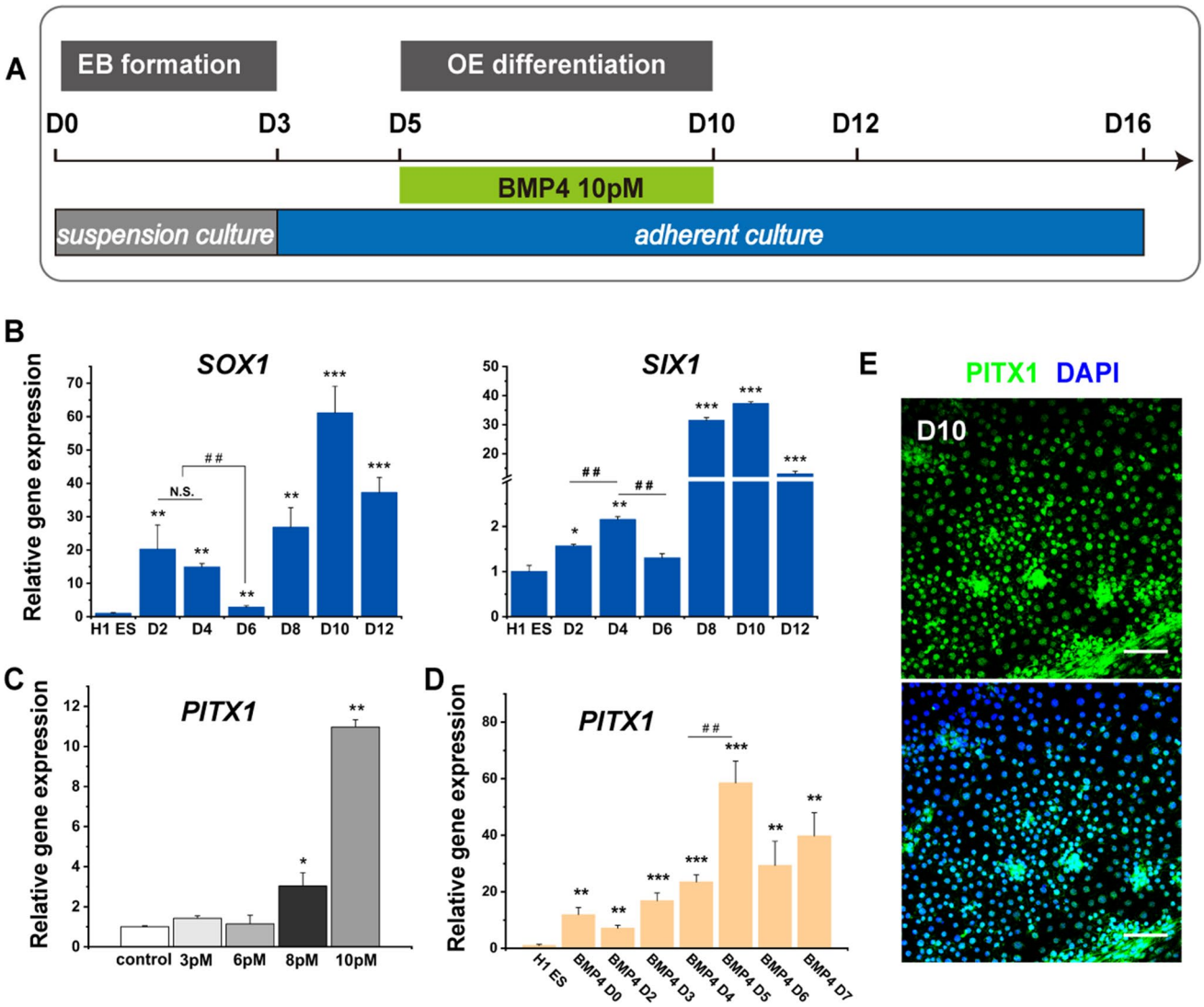

Fig. 1 Derivation of oral ectoderm from hPSCs. (**A**) EBs were formed in suspension culture condition for 3 days and then transferred to tissue-cultured plates for adherent cultures. BMP4 was added to induce OE differentiation from day 5 to day 10 at a final concentration of 10 pM. EBs, embryoid bodies; OE: oral ectoderm. (**B**) After EBs were transferred to tissue-cultured plates, adherent cells were harvested on different time point and qPCR was performed to examine the expression of neural ectoderm (SOX1) and non-neural ectoderm (SIX1). Data are presented as means ± S.D., and were normalized to GAPDH in three independent experiments. The results are reported as the fold change compared to H1 ES (*) and to each other (#). N.S.: not significant. *: $p<0.05$, ** and ##: $p<0.01$, ***: $p<0.001$ by unpaired, two-tailed Student's t test. (**C**) qPCR revealed PITX1 expression (OE marker) when BMP4 (3, 6, 8 or 10 pM) was added to the cultures from day 5 to day 10. Data are presented as means ± S.D. and were normalized to GAPDH in three independent experiments. The results are reported as the fold change compared to controls (cells cultured without BMP4). *: $p<0.05$, **: $p<0.01$, by unpaired, two-tailed Student's t test. (**D**) qPCR revealed the expression of PITX1 after adherent cells were treated with BMP4 for several days. Data are presented as means ± S.D., and were normalized to GAPDH in three independent experiments. The results are reported as the fold change compared to H1 ES (*) and to each other (#). ** and ##: $p<0.01$, ***: $p<0.001$ by unpaired, two-tailed Student's t test. (**E**) Immunofluorescence staining revealed PITX1 was expressed at day 10 of the differentiation. Scale bars: 100 μm

In this study, we developed an efficient method for generation of human salivary gland epithelial progenitors (SGEPs) from hPSCs, including hESCs and hiPSCs. Briefly, we first induced OE differentiation using an improved protocol. RA was then used to promote the SG initial differentiation, followed by 4-day CHIR99021 treatment to activate Wnt signaling for facilitating the specification of SGEPs. The hPSCs-derived SGEPs expressed progenitor markers, such as SOX9, KRT5, and KRT19, characteristic of mouse embryonic SMGs. We also found CD24 and α-SMA positive cells in SGEPs, which are known to have regeneration potential after injury. Importantly, the RNA-sequencing analysis demonstrated that the SGEPs had similar transcriptome profile to human fetal SMGs.

Materials and Methods

Human Pluripotent Stem Cell Maintenance and SGEP Differentiation

The hESC lines H1 and H9 were kindly provided by WiCell Research Institute (Madison, Wisconsin). The hiPSC line hNF-C1 was provided by Guangzhou Institutes of Biomedicine and Health (Guangzhou, China). Undifferentiated hPSCs were maintained in serum-free mTeSR1 medium (STEMCELL) and on Matrigel™ (1:160 dilution) coated plates. Passaging was performed every 4 days using 0.5 mM EDTA as a cell dissociation reagent. SGEP differentiation started with EB formation. hPSCs colonies were isolated using 1 mg/ml Dispase II and the cell aggregates were plated in low-cell adhesion plates (day 0). The differentiation medium was DMEM/F12 medium with 10% knockout serum replacement, 1.5% FBS, 1 mM GlutaMAX, 2 mM NEAA, 1 mM Penicillin-streptomycin and 0.14 mM 2-Mercaptoethanol. EBs were harvested on day 3 and transferred to tissue-treated cell culture plates at a ratio of 1:3 to allow cell adherence for 2 additional days without disturbing. To induce OE differentiation, cells were cultured in differentiation medium plus 10 pM BMP4 from day 5 to day 10. RA was applied to the cultures on day 10 for 2 days at a final concentration of 1 μM, followed by a 4-day treatment of 6 μM CHIR99021 to induce SGEP specification. The fresh medium was changed every 2 days.

Mouse and Human SMG Isolation

The mouse embryonic SMGs were isolated using a previously published protocol [18]. Ameloblastoma patients participated in this study after providing written informed consent in accordance with ethical guidelines. Healthy SMGs were collected during the intraoral microvascular anastomosis. Harvested samples were fixed in 4% paraformaldehyde (PFA) and equilibrated in 30% sucrose to allow them to sink to the tubes' bottom. Samples were then embedded in optical coherence tomography, and cryo-sectioned at a thickness of 10 μm for immunofluorescence staining.

Immunofluorescence Staining

To perform immunofluorescence staining, cells were fixed in 4% paraformaldehyde (PFA) for 30 minutes at room temperature or overnight at 4 °C. The cells or sections were treated with 0.1% Triton X-100 at room temperature for 10 minutes, and blocked in 3% BSA for 2 hours at room temperature. Primary antibodies were diluted in the blocking solution and added to the samples overnight at 4 °C. After washing three times with PBS, cells were incubated with secondary antibodies (diluted in PBS) for 1 hour at room temperature, followed by staining with DAPI (1 μg/ml) and observed using a NIKON A1R-si confocal microscope.

RNA Extraction and qPCR

Total RNA was isolated using the TRIZOL reagent. Reverse transcription was performed using the RevertAid First Strand complementary DNA Synthesis Kit, according to the manufacturer's instructions. The mRNA expression levels were measured by quantitative real-time polymerase chain reaction (qPCR) using SybrGreen master mix (Roche) as follows: predenaturation at 95 °C for 10 min, followed by 40 cycles of 95 °C for 5 s and 60 °C for 30 s.

Flow Cytometry

For flow cytometry, cells were incubated with 0.25% Trypsin-EDTA and sprayed to single cells. After fixation in 1% PFA for 15 minutes and permeabilized with 0.1% Triton X-100 or 0.2% Tween-20 for 10 minutes, the cells were incubated with primary antibody for 45 minutes at 4 °C, followed by the second antibody for 15 minutes. Cells were then resuspended in PBS and passed through a 40 μm cell strainer. Stained cells were analyzed using the BD Fortessa SORP (BD Biosciences, San Jose, CA, USA), and data were measured using the FlowJo software (Ashland, Oregon).

RNA Sequencing and Analysis

For RNA sequencing (RNA-seq), total RNA was extracted from H1 ES-derived SGEPs on day 16 using Rneasy mini kit (Qiagen), according to the manufacturer's instructions. RNA concentration and quality were measured using NanoDrop 2000 (Thermo Fisher Scientific, Wilmington, DE) and the Agilent Bioanalyzer 2100 system (Agilent Technologies, CA, USA). Sequencing libraries were prepared using NEBNext Ultra™ RNA Library Prep Kit for Illumina

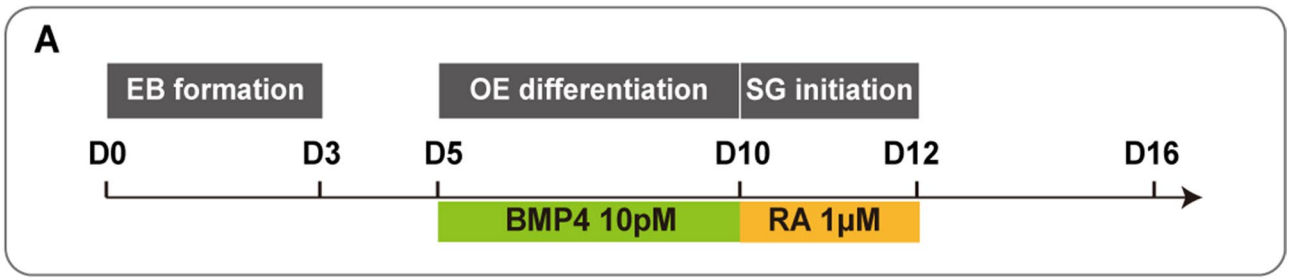
A
EB formation
OE differentiation
SG initiation
D0
D3
D5
D10
D12
D16
BMP4 10pM
RA 1μM

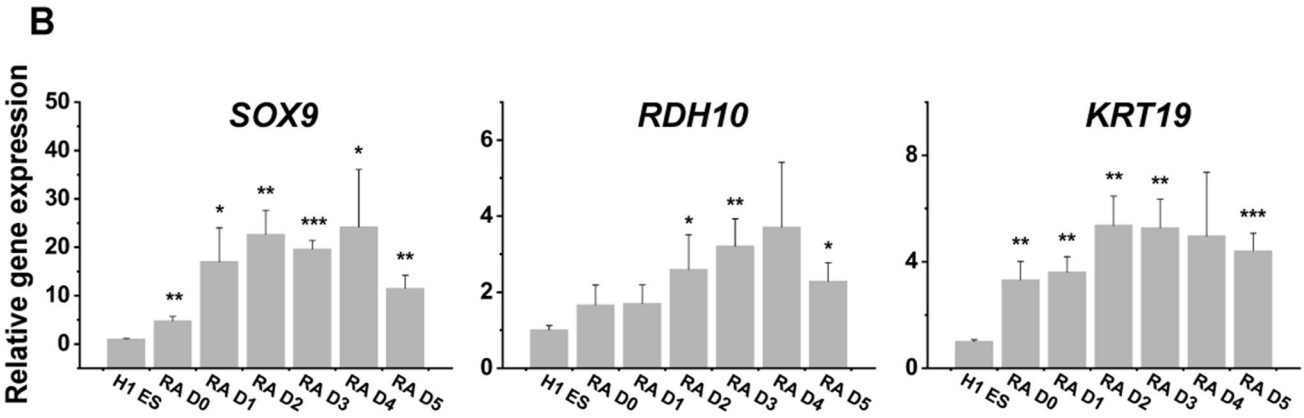
B
Relative gene expression
SOX9
RDH10
KRT19
H1 ES
RA D0
RA D1
RA D2
RA D3
RA D4
RA D5

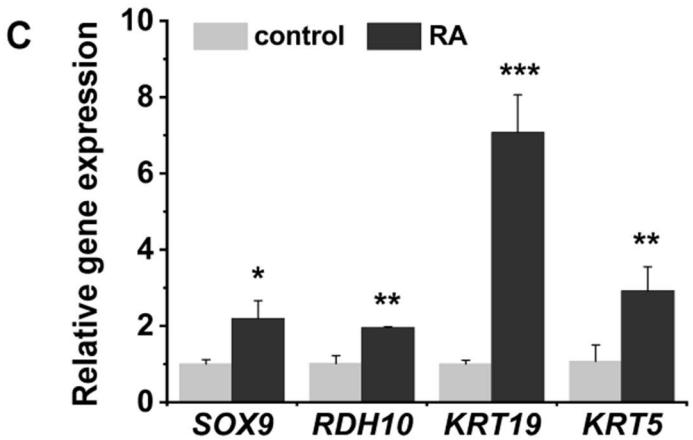
C
control
RA
Relative gene expression
SOX9
RDH10
KRT19
KRT5

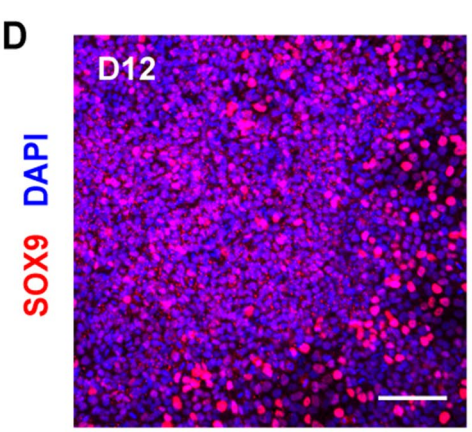
D
D12
SOX9
DAPI

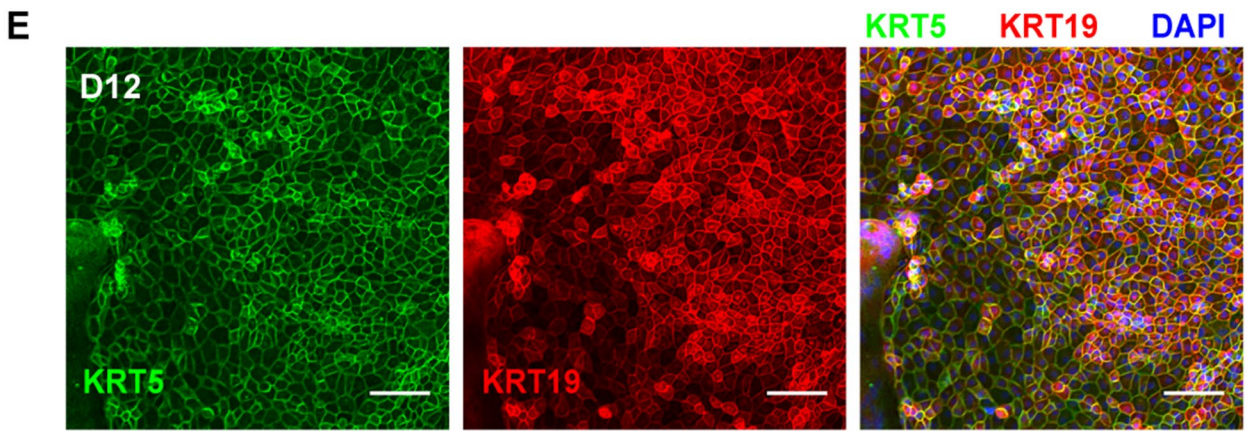
E
D12
KRT5
KRT19
KRT5
KRT19
DAPI

◂**Fig. 2** Induced of the SG progenitor initial differentiation by RA. (**A**) hESCs derived OE cultures were treated with RA in a final concentration of 1 μM for 2 days. EBs, embryoid bodies; OE: oral ectoderm. SG: salivary gland. (**B**) qPCR revealed the expression of specific markers after OE cultures were treated with RA for several days. Data are presented as means ± S.D. and were normalized to GAPDH in three independent experiments. The results are reported as the fold change compared to H1 ES. *: $p<0.05$, **: $p<0.01$, ***: $p<0.001$, by unpaired, two-tailed Student's t test. (**C**) RA was added to the OE cultures, and the mRNA expression of SOX9, RDH10, KRT19 and KRT5 was examined using qPCR on day 12 of differentiation. Data are presented as means ± S.D. and were normalized to GAPDH in three independent experiments. The results are reported as the fold change compared to controls (cells cultured without RA). *: $p<0.05$, **: $p<0.01$, ***: $p<0.001$, by unpaired, two-tailed Student's t test. (**D-E**) Immunofluorescence staining showed the expression of SOX9 (**D**), KER5 (**E**), and KRT19 (**E**) at day 12 of differentiation. Scale bars: 100 μm

(NEB, USA), following the manufacturer's recommendations, and index codes were added to attribute sequences to each sample. Sequencing was performed on Illumina Novaseq 6000 platform and paired-end reads were generated. Quality-controlled clean data was generated and then mapped to the reference genome (GRCh38_release95) using Hisat2. Quantification of gene expression levels was measured by fragments per kilobase of transcript per million fragments mapped (FPKM). DESeq2 was used to perform differential expression analysis and genes with an adjusted p value <0.01 were considered as differentially expressed. RNA sequencing data from human fetal and adult SMGs were downloaded from GEO dataset (GSE143702).

Statistical Analysis

All quantitative values are shown as means ± standard deviation (SD) of three independent experiments. We used two-tailed, unpaired Student's t test to determine statistical significance. Multiple group comparisons were performed using one-way analysis of variance (ANOVA) followed by Tukey's multiple comparison test. Differences were considered significant at a p value of <.05, .01, and .001, respectively.

Results

Sequential Differentiation of hPSCs to Salivary Gland Epithelial Progenitors by RA and CHIR99021

Before differentiation, the pluripotency of hESCs was assessed, and the maintained OCT4 and NANOG expressions were found (Fig. S1A-B). To induce hESCs differentiation into oral ectoderm (OE), we developed an improved protocol based on our previous study (Fig. 1A) [19]. Briefly, the hES cell line, H1, were differentiated into embryoid bodies (EBs) in suspension condition for 3 days, and followed by 2-day adherent culture (Figs. 1B and S1C). As the expression of neural ectoderm decreased, non-neural ectoderm began to increase (Figs. 1B and S1D). BMP4 was then used to stimulate OE differentiation. The final concentration of BMP4 was selected and 10 pM was sufficient to promote the expression of PITX1. (Fig. 1C). Treatment of BMP4 for 5 days significantly increased the expression level of PITX1 (Fig. 1D). In addition, immunofluorescence staining and flow cytometry confirmed strong PITX1 expression on day 10 (Figs. 1E and S1E), indicating efficient OE generation.

RA signaling activity, present in developing mouse SMGs before and during initiation, is required to regulate the earliest stage of SMG initiation [16]. Wnt signaling maintains the end bud progenitors of mouse fetal SMGs in an undifferentiation state [17]. Next, we tested whether sequential activation of RA and Wnt signaling promoted the specification of OE toward SGEPs. OE was treated with RA for 2 additional days (Fig. 2A-B). The 2-day treatment was sufficient to increase the initial marker SOX9 and activate RA signaling, as indicated by RDH10 expression (Figs. 2C and 3D), consistent with the finding in mouse embryonic SMGs [16]. Prolonged the duration of RA treatment result in more cell debris and generation of cells with irregular morphology (Fig. S2A). The levels of KRT5 and KRT19, SMG duct progenitor markers, also increased after RA induction (Fig. 2C), suggesting that RA signaling may also regulate duct development in the initial stages of fetal SMGs. Immunofluorescence analysis also confirmed the expression of these markers on day 12 of differentiation (Fig. 2D-E). To mimic the development processes of embryonic SMGs, we next used CHIR99021 to activate Wnt signaling (Fig. 3A). We determined that the suitable final concentration of CHIR99021 was 6 μM, indicated by the higher level of AXIN2 and SMG markers (Fig. 3B). Lower expression of AXIN2 and no significant change or reduced expression of salivary progenitor markers when the concentration was 9 μM suggested that a high concentration of CHIR99021 inhibits WNT signaling, which may be due to the cytotoxicity (Fig. 3B). The 4-day treatment increased the expression level of AXIN2, demonstrating this condition can mimic the activity of the Wnt/β-catenin pathway, as well as the level of mouse SMG progenitor markers, including SOX9, KRT5, and KRT19 (Fig. 3B) [20, 21]. As differentiation proceeds, the cell cultures became condensed and generated cobblestone-like SGEPs, similar to our previously isolated human SMG progenitors (Figs. 3C and S2B). During SGEP differentiation, the transcript levels of pluripotent markers, OCT4, decreased concomitantly with increased expression of SOX9, KRT5, and KRT19 after sequential induction by RA and CHIR99021 (Fig. 3D). Notably, α-SMA also increased from day 10 to day 16 (Fig. 3D), consistent with the expression of α-SMA begins in mouse embryonic SMG and its increase during

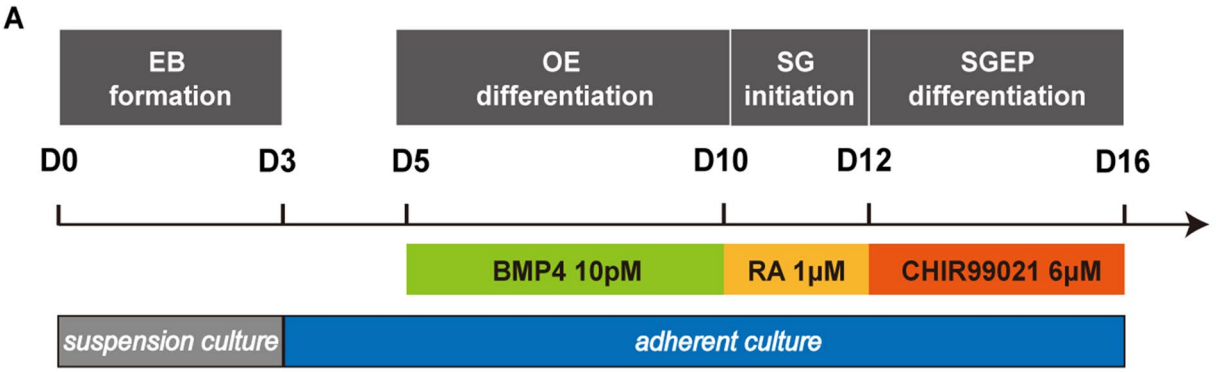
A
EB formation
OE differentiation
SG initiation
SGEP differentiation
D0
D3
D5
D10
D12
D16
BMP4 10pM
RA 1μM
CHIR99021 6μM
suspension culture
adherent culture

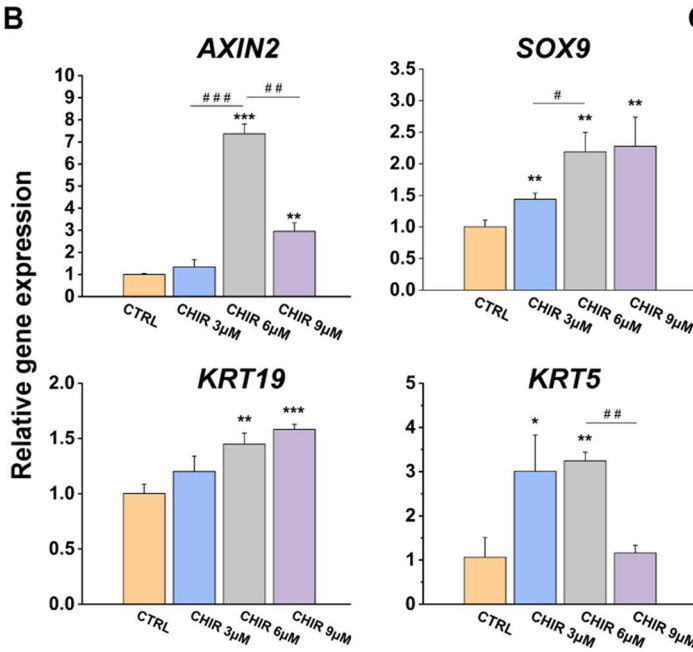
B
AXIN2
SOX9
KRT19
KRT5
Relative gene expression
CTRL
CHIR 3μM
CHIR 6μM
CHIR 9μM

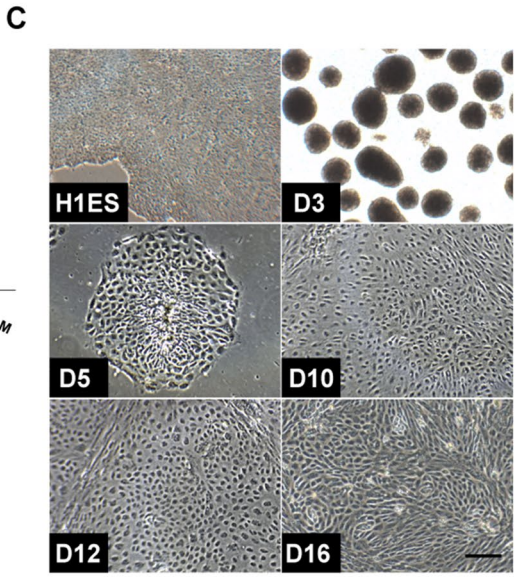
C
H1ES
D3
D5
D10
D12
D16

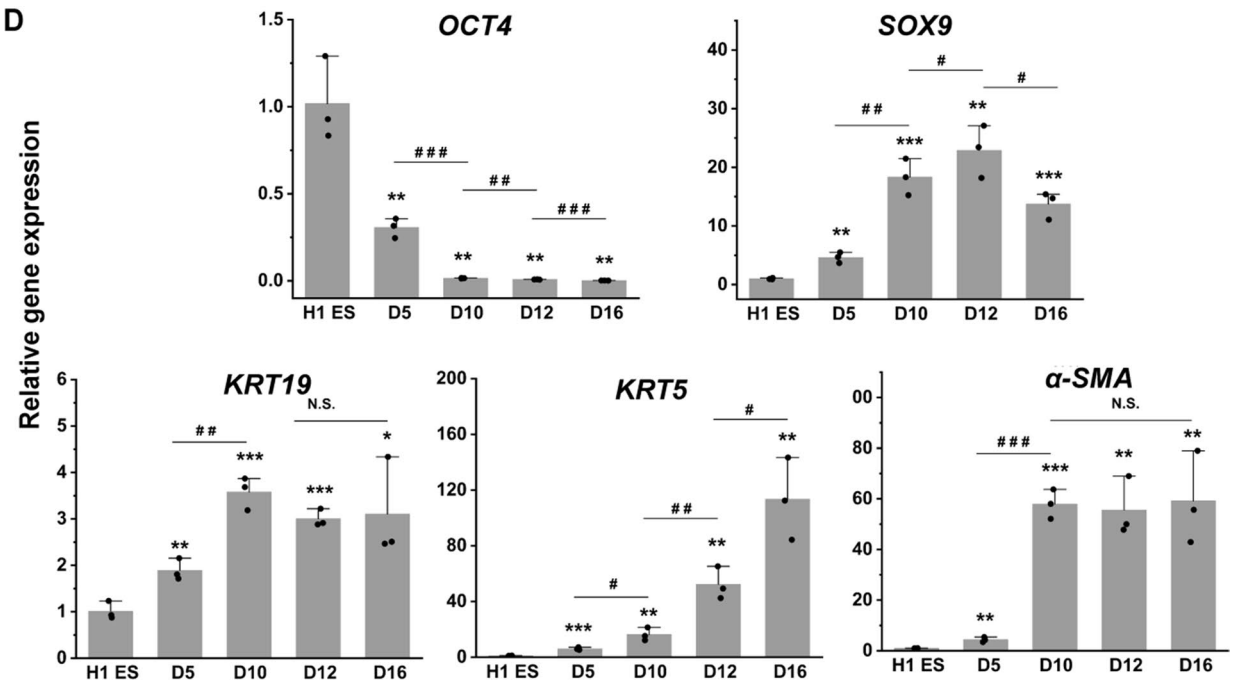
D
OCT4
SOX9
KRT19
KRT5
α-SMA
Relative gene expression
N.S.
H1 ES
D5
D10
D12
D16

◂**Fig. 3** Sequential differentiation of hESCs into SGEPs using RA and CHIR99021. (**A**). Protocol for derivation of hESC derived SGEPs by RA and CHIR99021. OE: oral ectoderm; SG: salivary gland. (**B**). CHIR99021 (3, 6 or 9 μM) was added to cultures, and the expressions of AXIN2 and progenitor markers were examined on day 16. Data are presented as means ± S.D., and were normalized to GAPDH in three independent experiments. The results are reported as the fold change compared to CTRL (control, cells cultured without CHIR99021, *) and to each other (#). * and #: $p < 0.05$, ** and ##: $p < 0.01$, *** and ###: $p < 0.001$, by unpaired, two-tailed Student's t test. (**C**) Bright-field images showed the morphology of the differentiating cells from day 0 to day 16. Scale bar: 200 μm. (**D**) qPCR revealed increased expression of SGEPs specific markers during differentiation. Data are presented as means ± S.D., and were normalized to GAPDH in three independent experiments. The results are reported as the fold change compared to H1 ES (*) and to each other (#). * and #: $p < 0.05$, ** and ##: $p < 0.01$, *** and ###: $p < 0.001$, by unpaired, two-tailed Student's t test. N.S.: not significant

development [22]. Taken together, this protocol efficiently promoted the differentiation of SGEPs from hPSCs.

hPSC-Derived SGEPs Expressed Markers that Are Characteristic of Developing Mouse Salivary Glands

We have shown that the hPSC-derived SGEPs expressed specific markers in mRNA level. Next, the protein expression levels of these markers were examined. Transcript factor SOX9 is present in the initial buds of mouse embryonic SMGs and was also expressed in the SGEPs (Fig. 4A and E) [13]. A major population (46%) of SOX9 positive epithelial cells was present on day 16 of differentiation (Fig. S3C). KRT5 and KRT19 are salivary specific duct progenitors in developing SMGs, and play essential roles in duct differentiation and homeostasis maintenance (Fig. 4E) [23, 24]. Immunofluorescence and flow cytometric analysis showed coexpression of these two markers in SGEPs on day 16 (Figs. 4B and S3C). Furthermore, these markers are also expressed in adult mouse and human SMGs, suggesting the efficient specification of SGEPs (Fig. S3A-B).

CD24 positive stem cells were found in adult mouse SMGs and showed the ability to repair the injured SMGs (Fig. S3A-B), which were also present in the hPSCs derived SGEPs (Fig. 4C) [25]. Moreover, α-SMA-positive cells were also found in SGEPs (Fig. 4D). The α-SMA positive myoepithelial cells are located around the acini of mature SMGs (Fig. 32A-B), contributing to acinar regeneration after severe and reversible glandular injury [26]. Previous studies have demonstrated that several populations of SG progenitor cells in embryonic stage not only give rise to tissues but also maintain and repair injured organ structures of adult SMGs [7]. Immunofluorescence analysis indicated that the mouse embryonic SMG epithelium expressed CD24 and α-SMA (Figs. 4E and S3C), indicating that these may serve as progenitor markers during development. These findings suggested that the hPSC-derived SGEPs mimicked mouse SG progenitors in the embryonic stage.

Derivation of SGEPs from hESCs Cell Line H9 and hiPSCs Cell Line hNF-C1

To determine whether SGEPs can be reproducibly generated from other hPSC cell lines, we used an hESC cell line H9 and a hiPSC cell line hNF-C1 to induce SGEP differentiation following the same protocol (Fig. 5A). Similarly, the H9 ES and hiPSCs derived SGEPs expressed increased transcript levels of SOX9, KRT5, KRT19, and α-SMA, while the pluripotent marker OCT4 decreased during differentiation (Figs. 5B and S4B).

Next, we examined the protein levels during SGEP specification, and immunofluorescence analysis revealed H9 and hiPSCs derived OE expressed a high level of PITX1 on day 10 (Fig. S4C). The expression of specific markers on day 12 had a pattern similar to that of H1 ES differentiation (Fig. S3D-G). As differentiation proceeded, both cell lines gave rise to SGEPs characterized by SOX9, KRT5, KRT19 expression on day 16 (Fig. 5C-D, F-G). Consistently, similar expression patterns were also observed for α-SMA and CD24, as in H1 ES-derived SGEP (Figs. 5E and H and S4H-I). Therefore, these data demonstrated the robustness and reproducibility of our protocol to induce various hPSC cell lines into SGEPs.

RNA-Seq Revealed the SGEPs Gene Expression Signature Is Similar to Human Fetal SMGs

To examine whether hPSCs derived SGEPs were similar to human SMGs, RNA-seq was performed to compare the SGEPs (day 16) gene expression profiles with the published dataset for human fetal and adult SMGs [27]. We first examined the expression level of genes specific to skin, neural ectoderm, endoderm and other epithelial/glandular tissues. And these data demonstrated that the hPSCs derived SGEPs showed a high correlation with transcriptomes of salivary glands (Fig. 6A). Differentially expressed genes and principal component (PCA) analysis revealed that the hSGEP gene expression profiles were relatively similar to those for human fetal SMGs (Figs. 6B and S5). Four clusters were within those genes, and we conducted Gene Ontology (GO) analysis to investigate the similarity between hSGEPs and fetal SMGs (Fig. 6C). The significant GO terms of genes highly expressed in both SGEPs and human fetal SMGs were related to salivary gland development, including biological processes including morphogenesis of an epithelium sheet, positive regulation of cell differentiation, and positive regulation of cell morphogenesis involved in differentiation (Fig. 6C, yellow panel). Notably, we also observed enrichment in Wnt signaling pathway in this cluster (Fig. 6C, yellow panel), suggesting the importance of Wnt activity during both SMG development and SGEP specification. Additionally, several genes were enriched in both SGEP and mature SMGs, which were related to sodium ion transport,

regulation of lipid metabolic process and organ regeneration (Fig. 6B-C, gray panels). These results were similar to the enriched GO annotation for neonatal SMGs [28]. There were two clusters that corresponded to genes specifically enriched in fetal (Fig. 6B, green panels) or adult SMGs (Fig. 6B, violet panels), respectively. Significant GO terms for genes uniquely expressed in human adult SMGs were associated with regulation of lipid metabolic process, sodium ion transport and protein transport ((Fig. 6C, violet panels)). These biological processes are essential for maintaining the secretion function of SMGs, indicating the SGEPs were progenitors and maintained in a less undifferentiation state. Genes enriched in human fetal SMGs were related to regulation of nervous system development, demonstrating the lacking of multiple system interaction during SGEP differentiation (Fig. 6C, green panels). A heatmap of key salivary gland genes revealed that the hPSCs derived SGEPs expressed multiple fetal SMG progenitor markers, including SOX9, KRT19, and SPRY2, but not mature SMGs such as CHRM1/3, AMY1A, and AQP5 (Fig. 6D), which is consistent with qPCR results (Fig. S6). Notably, RNA-seq data also revealed that α-SMA (ACTA2) and CD24 were expressed by both SGEPs and human fetal SMGs (Fig. 6D). These results confirmed that the hPSCs derived SGEPs had a similar gene expression signature to human fetal SMGs.

Discussion

In this study, we established an efficient protocol for differentiation of hPSCs into SGEPs based on the signaling involved in SMG development. The protocol was tested in three hPSC cell lines including two hESC and one hiPSC cell lines, and all of them can reproducibly give rise to SGEPs. hPSCs derived SGEPs expressed salivary progenitor markers, including SOX9, KRT5, and KRT19, as well as CD24 and α-SMA, which are characteristics of cell populations contribute to glandular regeneration. Moreover, the transcriptome analysis revealed that the SGEPs had gene expression profiles similar to human fetal SMGs.

We previously reported a protocol to induce the differentiation of OE from hPSCs [19]. In that protocol, EBs were generated and transferred to tissue-culture plates in a ratio of 1:1 to allow adherent cultures. However, seeding the EBs at high starting density inhibited the cell growth, especially under long-term differentiation, which was unsuitable for hPSCs derived SGEP generation. Therefore, in the present study we first optimized OE induction by diluting the seeding density to 1:3. We found that BMP4 treatment at 1 pM was insufficient to induce OE under this experimental condition, possibly due to reduced cell-cell communication. Higher BMP4 concentration efficiently facilitated OE differentiation from hPSCs, and subsequent experiments confirmed that the improved protocol for OE generation ensured the efficient specification of SGEPs. However, too high concentrations of BMP4 will result in non-specific differentiation [19].

We then developed the protocol for SGEP derivation by mimicking the activity of RA and Wnt signaling. RA treatment increased the level of SOX9 in SGEP differentiation, as observed in mouse models [15, 16]. Moreover, KRT5 and KRT19 were also up-regulated, both are considered as important cell populations for duct formation during SMG development [21], which suggests that RA may contribute to the biological process of SMG duct differentiation. Wnt signaling controls the timing of SMG development by maintaining the initial-bud progenitors in an undifferentiated state [17]. To recapitulate this process during in vitro SGEP specification, we used CHIR99021 to activate Wnt activity. The q-PCR analysis revealed that the expression of multiple progenitor markers was maintained or increased from day 12 to day 16. Therefore, together these results provided evidence that step-wise treatment of RA and CHIR99021 facilitated the SGEP differentiation from hPSCs.

The hPSCs derived SGEPs expressed high transcript and protein levels of SOX9, KRT5, and KRT19, progenitors during SG development. Previous studies have demonstrated that the entire SMG epithelium, including acinar and ducts, is derived from SOX9 positive progenitors, which are also present in the intercalated and striated ducts of adult mouse SMGs [13]. Lineage tracing assay revealed that the progeny of KRT5 positive epithelial progenitors was widespread in the SMG ductal and acinar compartments [24]. A trajectory inference analysis for single-cell RNA-seq of mouse embryonic, postnatal, and adult SMGs reveals that all other postnatal cell populations were derived from KRT19 positive duct cells, suggesting that KRT19 positive cells are a progenitor population in mouse fetal SMGs [20]. Moreover, KRT5-positive cells are progenitors of KRT19-positive cells and differentiate in such a manner. The basal KRT5-positive progenitor cells differentiate to the developing lumen, both positive for KRT5 and KRT19. As development proceeds, these progenitors lose the expression of KRT5. We also found SGEPs coexpressed KRT5 and KRT19 on day12 and day16 (Figs. 2E and 4B and S3C), as observed in mouse developing ducts. These results demonstrated that the combination of RA and CHIR99021 promoted the differentiation of KRT5 positive progenitors into developing ducts. We also found α-SMA and CD24 positive SGEPs during differentiation. A previous study isolated CD24 positive cells from mouse SMGs and demonstrated that these cells hold the potential to restore saliva secretion of injured SMGs. Moreover, α-SMA positive cells de-differentiate to progenitors in a bipotent state and re-differentiate into both AQP5 positive acini and KIT positive intercalated ducts after a severe injury [26]. CD24 and α-SMA were also observed in fetal mouse SMGs, suggesting they could be considered as

progenitors which maintain during adulthood. Overall, these findings confirmed that the hPSCs derived SGEPs mimic the characteristics of mouse SMG progenitors in embryonic stages. Additionally, these markers were expressed in at least three hPSC cell line derived SGEPs, including two hESC cell lines H1 and H9, and a hiPSCs cell line, hNF-C1. These results verify the robustness of our protocol, and its potential applications in future research.

Studies on human SG development are still lacking, and it remains unknown whether these progenitor markers above are also present in human fetal SMGs and the similarities between hPSCs derived SGEPs and human fetal SMGs. We did not obtain human fetal SMGs due to the complex ethical issues, but published RNA-seq datasets are available for these tissues [27]. The RNA-seq results revealed that SGEPs were similar to human fetal SMGs. Genes highly expressed in SGEPs and human fetal SMGs were associated with salivary organogenesis, as observed in fetal SMGs [28]. Moreover, significant GO terms for genes enriched in both SGEPs and mature SMGs were similar to those for neonatal SMGs, suggesting that the SGEPs had a tendency to differentiate to mature SG cells. Both hPSCs derived SGEPs and human fetal SMGs expressed a high level of SMG progenitor markers, as well

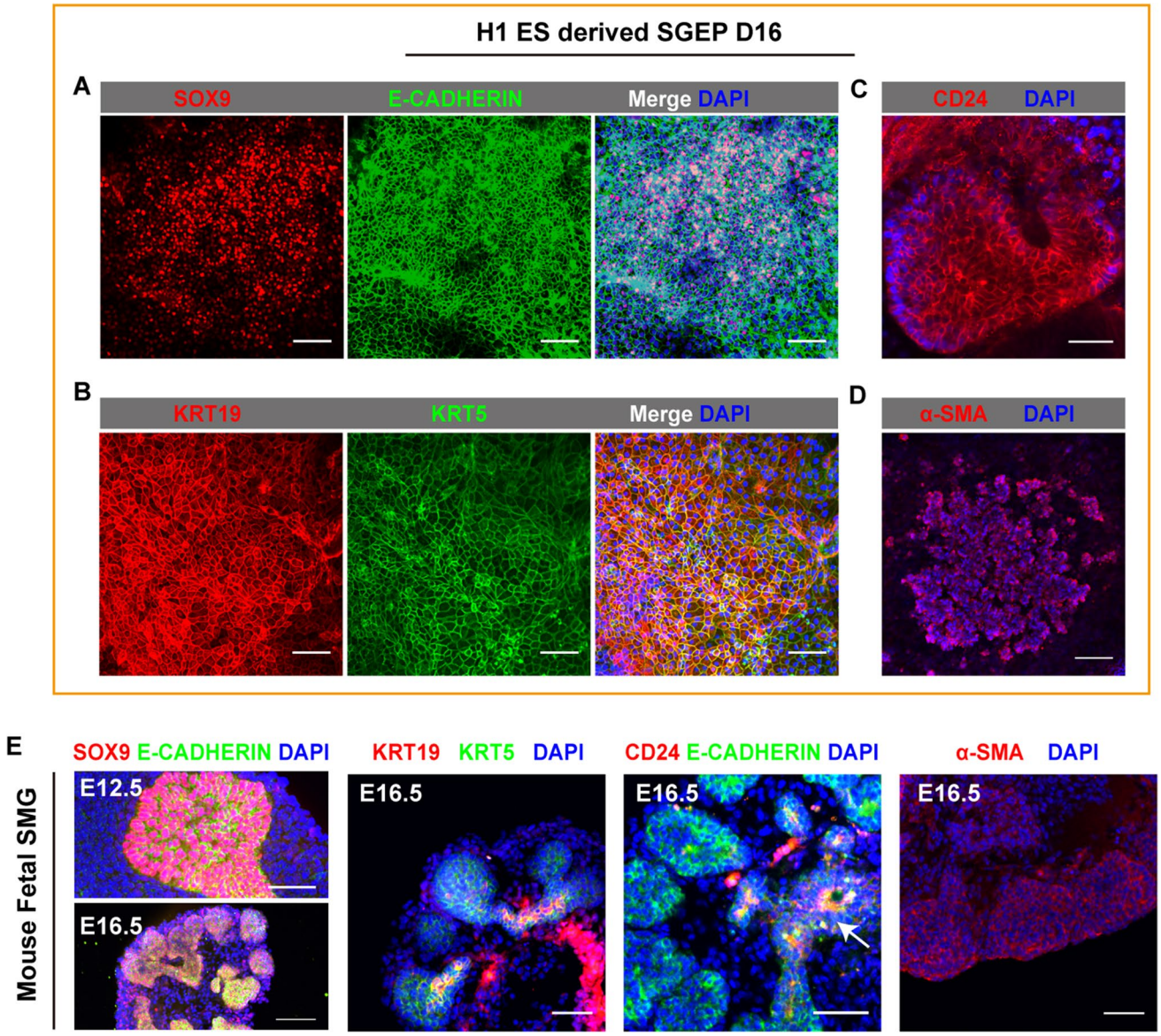

Fig. 4 H1 ES derived SGEPs expressed SMG progenitor markers. (**A-D**) Immunofluorescence staining revealed that human ESCs (H1 ES) derived SGEPs expressed multiple markers: SOX9 (**A**), KRT19, KRT5 (**B**), CD24 (**C**) and α-SMA (**D**) on day 16 of differentiation. Scale bars: 100 μm (**A-B**), 50 μm (**C**) and 200 μm (**D**). SGEPs: salivary gland epithelial progenitors. (**E**) Epithelium in E12.5 and E16.5 mouse SMGs expressed SOX9. Mouse embryonic SMGs (E16.5) expressed KRT5, KRT19, CD24 and α-SMA. Scale bars: 50 μm and 100 μm (E16.5). SMG: submandibular gland

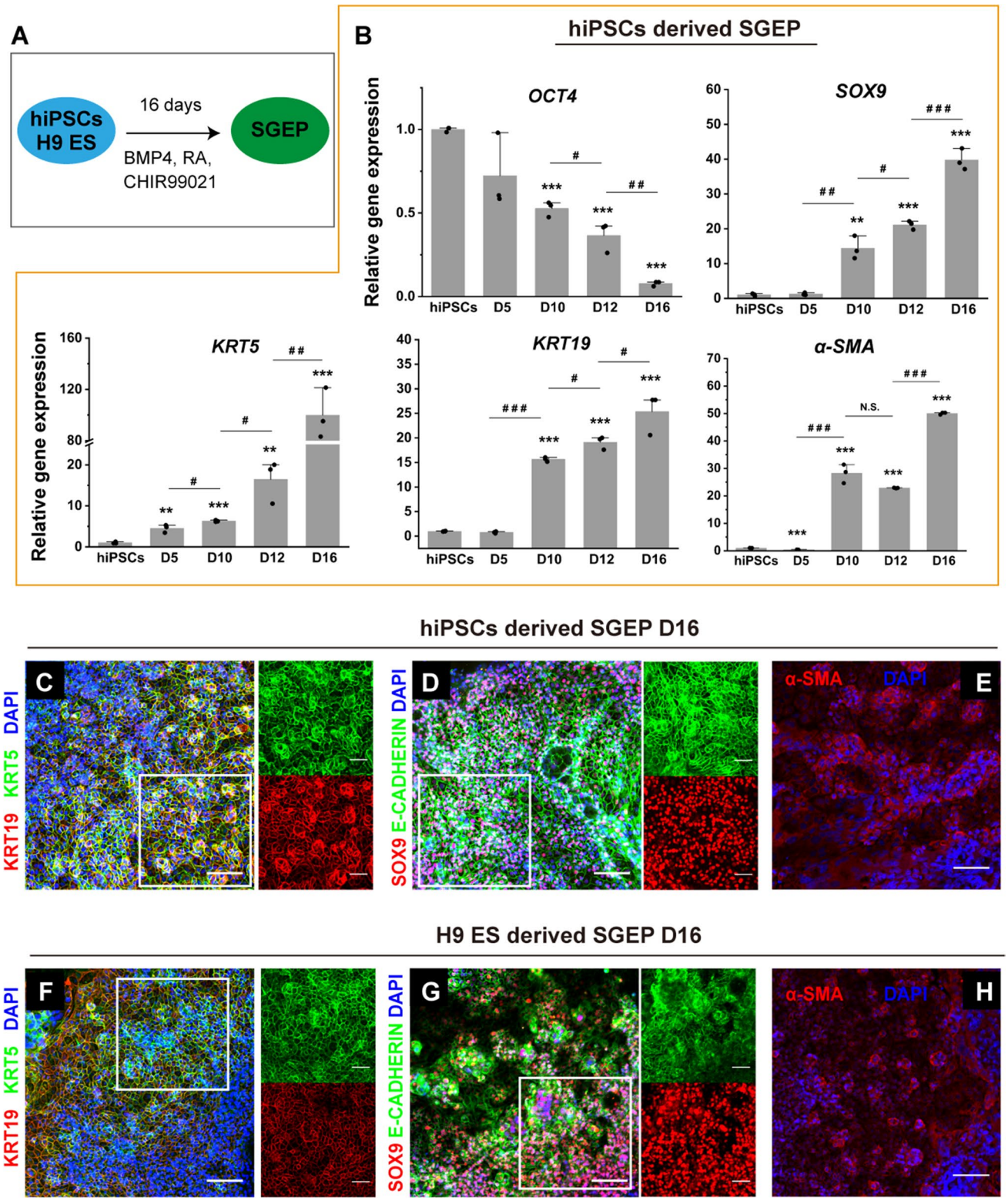

Fig. 5 Derivation of SGEPs from human iPSCs and H9 human ES cell lines. (**A**) SGEPs were generated from hiPSCs and H9 human ES cell lines following our protocol; (**B**) qPCR revealed increased expression of SG specific markers during differentiation of hiPSCs into SGEPs. Data are presented as the fold change compared with the mean ± S.D., and were normalized to GAPDH in three independent experiments. The results are reported as the fold change compared to hiPSCs (*) and to each other (#). * and #: $p < 0.05$, ** and ##: $p < 0.01$, *** and ###: $p < 0.001$, by unpaired, two-tailed Student's t test. N.S.: not significant. (**C-H**) Immunofluorescence staining showed that hiPSCs (**C-E**) and H9 ES (**F-H**) derived SGEPs expressed SMG progenitor markers: KRT5, KRT19 (**C**, **F**), SOX9 (**D**, **G**), α-SMA (**E**, **H**). Scale bars: 100 μm and 50 μm (magnified images, marked by white boxes)

as CD24 and α-SMA, consistent with the mouse counterparts. However, the hPSCs derived SGEPs are negative for markers involved in SG secretory function and also in a less undifferentiation state. Further studies should focus on investigating maturation factors during in vitro differentiation. In addition, our study demonstrated that the activity of these markers, and the RA and Wnt signaling were conserved between mice and humans. More importantly, we confirmed the characteristics of hPSCs derived SGEPs by comparing both mouse and human fetal SMGs, which provided convincing evidence for the remarkable applications in human research.

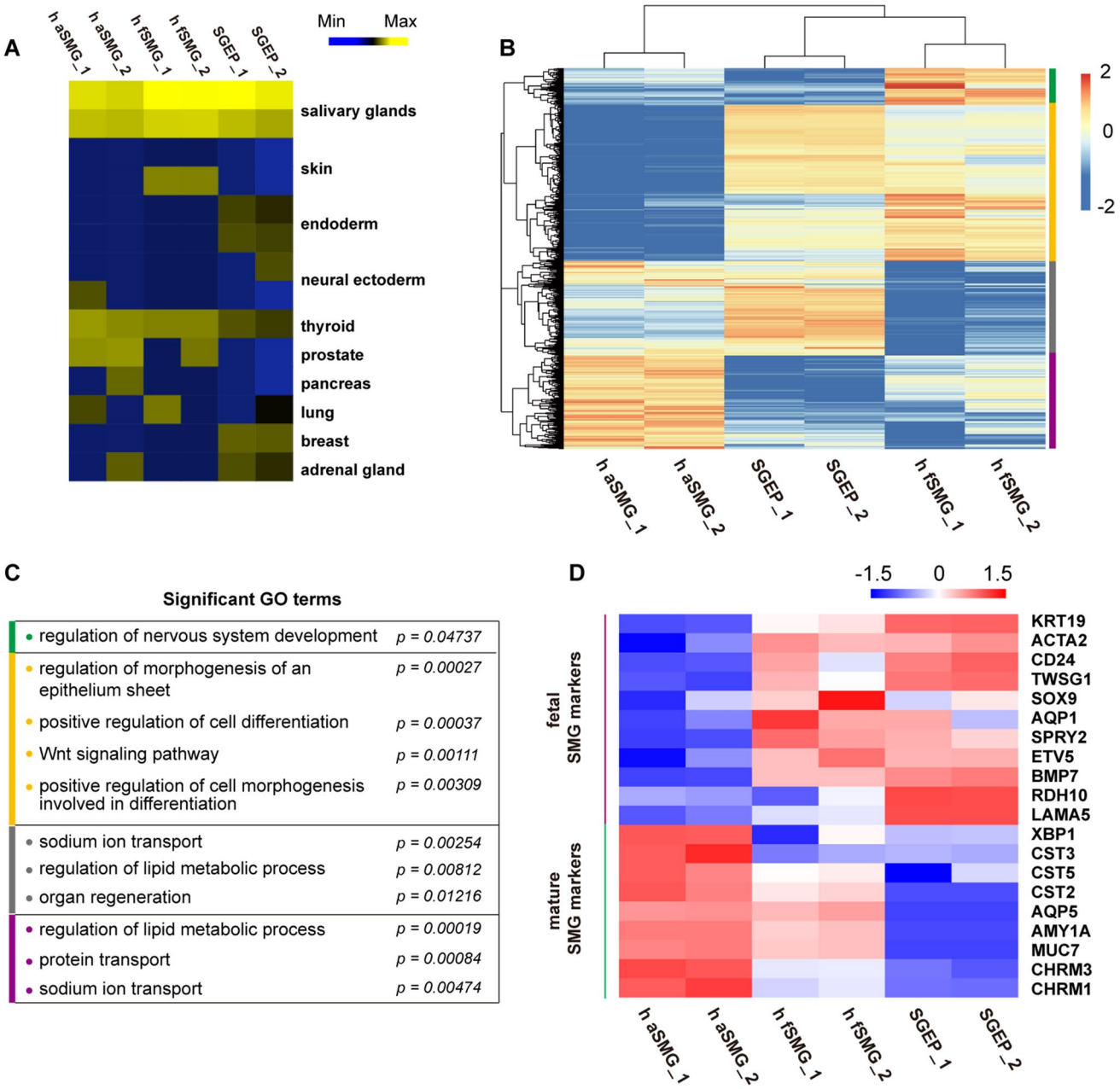

Fig. 6 hPSCs derived SGEPs had gene expression profile similar to human fetal SMGs. (**A**) A heatmap revealed the hPSCs derived SGEPs are negative for markers specific to other tissues, including skin, endoderm, neural ectoderm, thyroid, prostate, pancreas, lung, breast and adrenal gland. Min: minimum, Max: Maximum. (**B**) A hierarchical cluster analysis of differentially expressed genes between SGEPs, human fetal SMGs (h fSMG) and human adult SMGs (h aSMG). FDR (False Discovery Rate) < 0.01 FC (Fold Change) ≥ 2. (**C**) Significant Gene Ontology (GO) terms (biological processes) terms for differentially expressed genes represent in (**B**). p: *p* value <0.05. (**D**) A heatmap revealed expression profiles of key genes related to human SMG development and maturation. SMG: submandibular gland

In conclusion, sequential RA and CHIR99021 treatment efficiently promoted SGEP differentiation. hPSCs derived SGEPs had similar characteristics and transcriptome profiles to both mouse and human fetal SMGs. Therefore, this study described for the first time an efficient and robust approach to generating SGEPs from hPSCs, which provided the foundation for generating functional hPSCs derived salivary gland acinar cells and three-dimensional organoids.

Supplementary Information The online version contains supplementary material available at https://doi.org/10.1007/s12015-022-10431-y.

Acknowledgements We thank the professor. Duanqin Pei of the Guangzhou Institutes of Biomedicine and Health kindly provides the hiPS cell lines. We also thank the professor.Yuanyuan Zhang of the Wake Forest Institute for Regenerative Medicine forthe guidance of this work. Moreover, the authors thank National Center for Protein Sciences at Peking University in Beijing, China, for assistance with providing Roche qPCR equipment and Nikon A1R confocal microscopy photography.

Authors' Contributions Conceptualization: S.Z., J.X. and S.W.; Methodology: S.Z., S.Y. and C.D.; Investigation: S.Z., Y.Z. and Y.F.; Formal Analysis: Y.Z. and S.Y.; Verification: S.Z., Y.S, and S.W.; Writing – Original Draft: S.Z., Y.S.; Writing – Review & Editing: Y.S., Y.Z., J.X., and S.W.; Resources: S.Z., Y.F.; Supervision: S.Z., S.W., and J.X.; Project Administration: S.Z., S.W.; Funding Acquisition: J.X., S.W.

Funding This work was supported by Discipline Development Fund of School of Stomatology, Peking University.

Data Availability The data used in this article will be available from the authors on reasonable request.

Code Availability The RNA-seq data files in this paper have been deposited into Gene Expression Omnibus (GEO). The accession number is GEO: GSE198097.

Declarations

Ethics Approval This work involved isolation of embryonic mouse SMGs and adult human SMGs. All procedures performed in this study were reviewed and approved by the Biomedical Ethics Committee of Peking University in China. The permit number for the animal part is LA2021052. The permit number for the human part is 19093.

Consent to Participate The human salivary gland tissues were collected after obtaining informed consent from the donors.

Consent for Publication Not applicable.

Conflict of Interest No competing interests declared.

References

1. Zhang, Y., Yang, Y., Jiang, M., Huang, S. X., Zhang, W., Al, A. D., Danopoulos, S., Mori, M., Chen, Y. W., Balasubramanian, R., de Sousa, C., Lopes, S. M., Serra, C., Bialecka, M., Kim, E., Lin, S., Toste de Carvalho, A. L. R., Riccio, P. N., Cardoso, W. V., et al. (2018). 3D modeling of esophageal development using human PSC-derived basal progenitors reveals a critical role for notch signaling. *Cell Stem Cell, 23*(4), 516–29 e5.
2. Lungova, V., Chen, X., Wang, Z., Kendziorski, C., Thibeault, S., & L. (2019). Human induced pluripotent stem cell-derived vocal fold mucosa mimics development and responses to smoke exposure. *Nature Communications, 10*(1), 4161.
3. Huang, S. X. L., Islam, M. N., O'Neill, J., Hu, Z., Yang, Y.-G., Chen, Y.-W., Mumau, M., Green, M. D., Vunjak-Novakovic, G., Bhattacharya, J., & Snoeck, H.-W. (2014). Efficient generation of lung and airway epithelial cells from human pluripotent stem cells. *Nature Biotechnology, 32*(1), 84–91.
4. Matsumoto, R., & Takahashi, Y. (2021). Human pituitary development and application of iPSCs for pituitary disease. *Cellular and Molecular Life Sciences, 78*(5), 2069–2079.
5. Joy, D. A., Libby, A. R. G., & McDevitt, T. C. (2021). Deep neural net tracking of human pluripotent stem cells reveals intrinsic behaviors directing morphogenesis. *Stem Cell Reports, 16*(5), 1317–1330.
6. Lee, J., Rabbani, C. C., Gao, H., Steinhart, M. R., Woodruff, B. M., Pflum, Z. E., Kim, A., Heller, S., Liu, Y., Shipchandler, T. Z., Koehler, K., & R. (2020). Hair-bearing human skin generated entirely from pluripotent stem cells. *Nature, 582*(7812), 399–404.
7. Miho, O., & Takashi, T. (2017). Functional Salivary Gland Regeneration by Organ Replacement Therapy. *Salivary Gland Development and Regeneration: Advances in Research and Clinical Approaches to Functional Restoration*.(p. 193-203). Springer International Publishing.
8. Mattingly, A., Finley, J. K., Knox, S., & M. (2015). Salivary gland development and disease. *Wiley Interdisciplinary Reviews: Developmental Biology, 4*(6), 573–590.
9. Pedersen, A. M., Bardow, A., Jensen, S., & Beier, N. B. (2002). Saliva and gastrointestinal functions of taste, mastication, swallowing and digestion. *Oral Diseases, 8*(3), 117–129.
10. Mattingly, A., Finley, J. K., Knox, S., & M. (2015). Salivary gland development and disease. *Wiley Interdisciplinary Reviews Developmental Biology, 4*(6), 573–590.
11. Patel, V. N., Hoffman, M., & P. (2014). Salivary gland development: A template for regeneration. *Seminars in Cell & Developmental Biology, 25-26*, 52–60.
12. Athwal, H. K., Murphy 3rd, G., Tibbs, E., Cornett, A., Hill, E., Yeoh, K., Berenstein, E., Hoffman, M. P., & Lombaert, I. M. A. (2019). Sox10 regulates plasticity of epithelial progenitors toward secretory units of exocrine glands. *Stem Cell Reports, 12*(2), 366–380.
13. Chatzeli, L., Gaete, M., Tucker, A., & S. (2017). Fgf10 and Sox9 are essential for the establishment of distal progenitor cells during mouse salivary gland development. *Development, 144*(12), 2294–2305.
14. Tanaka, J., Ogawa, M., Hojo, H., Kawashima, Y., Mabuchi, Y., Hata, K., Nakamura, S., Yasuhara, R., Takamatsu, K., Irie, T., Fukada, T., Sakai, T., Inoue, T., Nishimura, R., Ohara, O., Saito, I., Ohba, S., Tsuji, T., & Mishima, K. (2018). Generation of orthotopically functional salivary gland from embryonic stem cells. *Nature Communications, 9*(1), 4216.
15. Wright, D. M., Buenger, D. E., Abashev, T. M., Lindeman, R. P., Ding, J., Sandell, L., & L. (2015). Retinoic acid regulates embryonic development of mammalian submandibular salivary glands. *Developmental Biology, 407*(1), 57–67.
16. Metzler, M. A., Raja, S., Elliott, K. H., Friedl, R. M., Tran, N. Q. H., Brugmann, S. A., Larsen, M., Sandell, L., & L. (2018). RDH10-mediated retinol metabolism and RARalpha-mediated retinoic acid signaling are required for submandibular salivary gland initiation. *Development, 145*(15), dev164822.

17. Matsumoto, S., Kurimoto, T., Taketo, M. M., Fujii, S., & Kikuchi, A. (2016). The WNT/MYB pathway suppresses KIT expression to control the timing of salivary proacinar differentiation and duct formation. *Development, 143*(13), 2311–2324.
18. Miho, O., & Takashi, T. (2017). Functional Salivary Gland Regeneration. *Organ Regeneration: 3D Stem Cell Culture & Manipulation*. (p. 135-51). Springer New York.
19. Li, Q., Zhang, S., Sui, Y., Fu, X., Li, Y., & Wei, S. (2019). Sequential stimulation with different concentrations of BMP4 promotes the differentiation of human embryonic stem cells into dental epithelium with potential for tooth formation. *Stem Cell Research & Therapy, 10*(1), 276.
20. Hauser, B. R., Aure, M. H., Kelly, M. C., Genomics, Computational Biology Core, Hoffman, M. P., & Chibly, A. M. (2020). Generation of a single-cell RNAseq atlas of murine salivary gland development. *iScience, 23*(12), 101838.
21. Knox, S. M., Lombaert, I. M. A., Reed, X., Vitale-Cross, L., Gutkind, J. S., Hoffman, M., & P. (2010). Parasympathetic innervation maintains epithelial progenitor cells during salivary organogenesis. *Science, 329*(5999), 1645–1647.
22. National Institute of Dental and Craniofacial Research (2011). [online] Available at: https://sgmap.nidcr.nih.gov/sgmap/sgexp.html. [cited 12 Nov. 2021].
23. Nedvetsky, P. I., Emmerson, E., Finley, J. K., Ettinger, A., Cruz-Pacheco, N., Prochazka, J., Haddox, C. L., Northrup, E., Hodges, C., Mostov, K. E., Hoffman, M. P., Knox, S., & M. (2014). Parasympathetic innervation regulates tubulogenesis in the developing salivary gland. *Developmental Cell, 30*(4), 449–462.
24. Knox, S. M., Lombaert, I. M. A., Reed, X., Vitale-Cross, L., Gutkind, J. S., Hoffman, M., & P. (2010). Parasympathetic innervation maintains epithelial progenitor cells during salivary organogenesis. *Science (New York, N.Y.), 329*(5999), 1645–1647.
25. Nanduri, L. S., Baanstra, M., Faber, H., Rocchi, C., Zwart, E., de Haan, G., van Os, R., & Coppes, R. P. (2014). Purification and ex vivo expansion of fully functional salivary gland stem cells. *Stem Cell Reports, 3*(6), 957–964.
26. Ninche, N., Kwak, M., & Ghazizadeh, S. (2020). Diverse epithelial cell populations contribute to the regeneration of secretory units in injured salivary glands. *Development, 147*(19), dev192807.
27. Saitou, M., Gaylord, E. A., Xu, E., May, A. J., Neznanova, L., Nathan, S., Grawe, A., Chang, J., Ryan, W., Ruhl, S., Knox, S. M., & Gokcumen, O. (2020). Functional specialization of human salivary glands and origins of proteins intrinsic to human saliva. *Cell Reports, 33*(7), 108402.
28. Gluck, C., Min, S., Oyelakin, A., Smalley, K., Sinha, S., Romano, R., & A. (2016). RNA-seq based transcriptomic map reveals new insights into mouse salivary gland development and maturation. *BMC Genomics, 17*(1), 923.

Publisher's Note Springer Nature remains neutral with regard to jurisdictional claims in published maps and institutional affiliations.

Springer Nature or its licensor holds exclusive rights to this article under a publishing agreement with the author(s) or other rightsholder(s); author self-archiving of the accepted manuscript version of this article is solely governed by the terms of such publishing agreement and applicable law.